SPECTROSCOPIC IDENTIFICATION AND CLASSIFICATION OF TERRAIN UNITS ON DIONE'S AND RHEA'S SURFACES BASED ON CASSINI/VIMS DATA. F. Scipioni[1], F. Tosi[1], M. Ciarniello[1], F. Capaccioni[1], G. Filacchione[1], K. Sthephan[2] and P. Cerroni[1], [1]INAF-IAPS, Istituto di Astrofisica e Planetologia Spaziali, Via del Fosso del Cavaliere 100, I-00133 Rome, Italy (francesca.scipioni@ifsi-roma.inaf.it), [2]DLR, Institute of Planetary Research, Rutherfordstrasse 2, 12489 Berlin, Germany.

Introduction: Since July 2004, the Cassini spacecraft performed several observations of Saturn's icy satellites, allowing a better insight of their compositional and physical characteristics.

With a diameter of 1122 km and a density of ρ = 1.475 g/cm^3, Dione is the second largest inner moon of Saturn and the third densest after Enceladus and Phoebe. The Voyager spacecrafts observed Dione in 1980 showing a complex surface structure, with both heavily cratered terrains and less cratered plains [1, 2]. Subsequently Dione was observed by the Cassini spacecraft in its nominal and extended. Most of Dione' surface is covered by the heavily cratered terrains, located mainly in the trailing hemisphere and crossed by high-albedo wispy streaks that are likely tectonic features [4].

Rhea is one of the largest and less dense moons of Saturn, with a diameter of 1528 km [3] and a density equal to 1.233 g/cm^3. The Voyager spacecraft was the first to observe Rhea' surface, revealing a complexity comparable to Dione [2]. Rhea's trailing side appears brighter than the leading side, with high albedo filaments similar to Dione's wispy streaks, possibly formed after resurfacing processes [5].

Data set and analysis: The Visual and Infrared Mapping Spectrometer (VIMS) instrument onboard the Cassini Orbiter is able to acquire hyperspectral images ("cubes") in the overall spectral range from 0.35 to 5.1 µm. In this work, we have selected 133 VIMS cubes of Dione and 68 cubes of Rhea in the infrared range 0.85-5.1 µm. These data are characterized by a phase angle smaller than 50° and a good S/N ratio (essentially driven by the exposure time).

After normalizing all data at λ=2.232 µm to minimize photometric effects, we have applied the supervised Spectral Angle Mapper (SAM) clustering technique to emphasize the existence of spectral units on the basis of their spectral properties.

The first step in this classification work has been to look for some reference spectra, or *endmembers*, to be compared with the other spectra of the two satellites produced by VIMS. Endmembers have been chosen by applying the *k-means* clustering method to Dione's and Rhea's cubes showing the highest spatial resolution. Nine endmembers for Dione (**Fig. 1**, top panel) and eight endmembers for Rhea (**Fig. 1**, bottom panel) have been identified. Each spectral unit is coded by a color. Then, the classification of all pixels belonging to all Dione's and Rhea's cubes has been performed through the Spectral Angle Mapper (SAM) classification method.

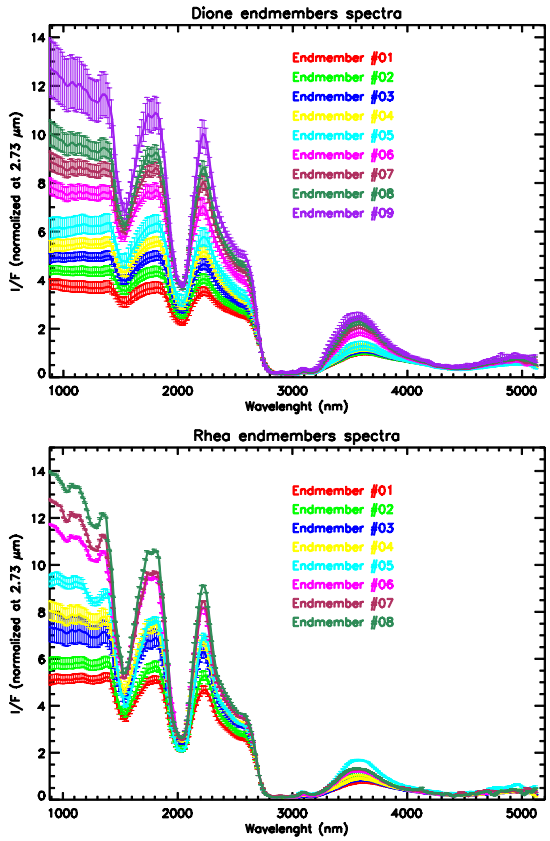

Figure 1: Dione's (**top panel**) and Rhea's (**bottom panel**) endmember spectra. Each endmember is coded by a color.

Results: To summarize the result of the SAM classification and compare them with the geological features on the surfaces of the satellites, we projected classified cube's pixels on a Dione's cylindrical map (**Fig. 2**, top panel) and on a Rhea's cylindrical map (**Fig. 2**, bottom panel). For the two satellites, the obtained homogeneous classes show differences in terms of water ice abundance and ice grain size.

For both satellites, the infrared spectrum is dominated by the prominent signatures of H_2O ice /OH bands at 1.5, 2.0 and 3.0 µm. For Rhea, the spectral signatures due to water ice at 1.04 and 1.25 µm are observed across the entire surface, while for Dione these spectral features are observed only on limited regions of the surface. Generally, the spectral classes classifying optically darker terrains are those showing

suppressed water ice bands and a higher concentration of carbon dioxide. Conversely, spectral units which label brighter regions have deeper water ice absorption bands, a higher albedo and a small abundance of CO_2.

In particular, Dione's dark terrain has been classified with spectral units #1 and #2, displaying the highest concentration of carbon dioxide (5% and 5.6%, respectively) and the most suppressed water ice absorption bands. Moreover, absorption bands at 1.04 and 1.25 μm, which can be used to trace pure water ice, do not show up. The wispy structures have been classified with spectral units #3 and #4. Also these classes show a CO_2 concentration higher than the following units (~ 4.8%) and the absence of the 1.04 and 1.25 μm bands. The passage between the trailing and the leading hemispheres is marked by units #6 and #7. The latter, together with unit #8, completely classifies the leading hemisphere. On these two units, the 1.04 and 1.25 μm absorptions show up, even though they are shallow. Moreover, water ice absorption bands at 1.5 and 2.0 μm become deeper and the CO_2 relative abundance decrease until ~ 4%. Finally, spectral class #9 concentrates only on a Dione's region located in the northern part of the leading hemisphere and which correspond to the Creusa (49°*N*, -76°*E*) impact crater region, one of the youngest satellite's terrains.

For Rhea, the asymmetry between the two hemispheres is less pronounced, even though the trailing hemisphere looks slightly darker than the leading hemisphere. The first four spectral units identified for Rhea classify both hemispheres, while classes from #5 to #8 concentrate only in the Inktomi crater region (12.5°*S*, -112°*E*) on the leading hemisphere. Inktomi is the youngest morphological structure known on Rhea' surface. The trailing hemisphere is mainly classified by spectral classes #1 and #3, while the leading hemisphere is mostly represented by classes #2, #3 and #4. Since we have less Rhea data than Dione data matching our selection criteria, and the spatial resolution is also lower, the agreement between morphological structures and variations in absorption band depths is less evident for Rhea than for Dione. Spectral units #7 and #8 label the Inktomi crater terrains, while the surrounding terrain gradually passes from units #6 to #4 with increasing distance from the crater. Units #7 and #8 characterize terrains with the purest water ice, since they show relatively deep absorptions at 1.04 and 1.25 μm and a low concentration of contaminants. For Rhea, absorptions at 1.04 and 1.25 μm are seen in all spectral units, even though the depth decreases from unit #8 to #1. The relative abundance of carbon dioxide is constant across Rhea' surface (~ 5%) and it decreases only for spectral units #6 and #8.

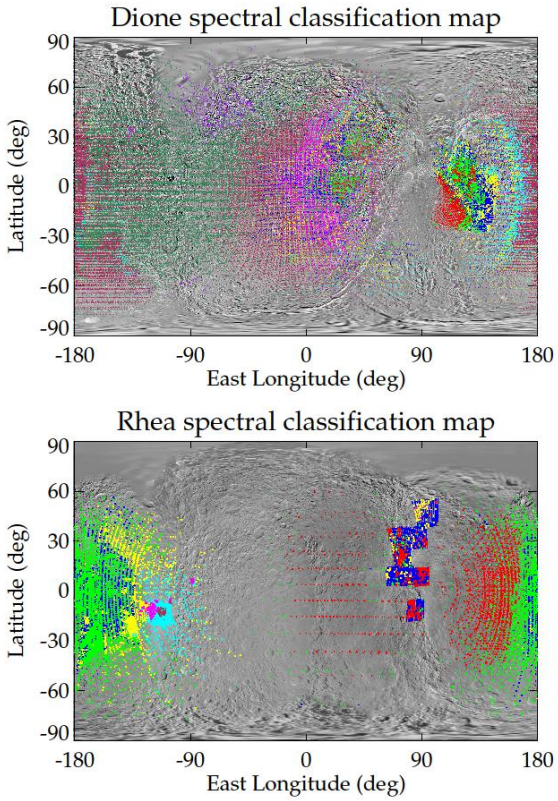

Figure 2: Projection of classified VIMS cubes' pixels on a Dione's cylindrical map (**Top panel**) and on a Rhea's cylindrical map (**Bottom panel**).

Conclusions: The classification method developed in this work allows us to relate spectral variations and morphological structures.

From our analysis we have found that: (1) ice grains sizes on Dione's and Rhea's surface must be larger than 25 μm; (2) the presence of contaminants is higher on Dione's and Rhea's trailing hemispheres; (3) wispy terrains are darker and more contaminated than leading hemisphere's terrains; (4) Creusa on Dione and Inktomi on Rhea, are the geologic features showing the highest amount of fresh, non-contaminated water ice.

Moreover, CO_2 concentrates mostly on Dione's dark terrains on the trailing hemisphere, but it is observed across its entire surface. CO_2 abundance is constant across Rhea's surface, but is lower compared with Dione, indicating that darkening mechanisms are more effective on Dione than on Rhea.

References: [1] Plescia, J. B., and Boyce, J. M., 1982, Nature 295, 285. [2] Smith, B. A., et al., 1981, Science 212, 163. [3] Stephan, K., et al., 2012, Planetary and Space Science 61, 142. [4] Wagner, R. J., et al., 2005, Bull. Am. Astron. Soc. 37 (3), 701 (Abstr. 6-02). [5] Wagner, R. J., et al., 2008, Lunar and Planetary Science XXXIX v. (Abstr. 1930).